JOURNAL OF MATERIALS SCIENCE 18 (1983) 1666–1674

Comparative study of the temperature dependence of hardness and compressive strength in ceramics

JAMES LANKFORD
Department of Materials Sciences, Southwest Research Institute, San Antonio, Texas 78284, USA

Hardness and compressive strength of several strong ceramics are measured from room temperature to 1000° C. Similarities in behaviour, and the results of microscopic examination, are interpreted in terms of the relative contributions of microplasticity and microfracture to material failure during compression testing and microhardness indentation. It is shown that microplasticity alone is an insufficient basis upon which to relate material response under the two test conditions, and that tensile microfracture is a significant contributor both to compressive failure and to subsurface indentation deformation, hence to hardness.

1. Introduction

More than a decade ago, Rice suggested [1] that the hardness and compressive strength of ceramics might be closely coupled through microplasticity. In support of this idea, extensive data from many sources were assembled and reviewed, leading to the conclusion that the yield stress, equal to one third of the microhardness, should be the upper limit of both ambient and elevated temperature compressive strength. Unfortunately, most of the available information involves the work of different investigators, using different materials and procedures.

The present research was undertaken to try and better define the physical damage processes which might link hardness and compressive strength. Therefore, experiments have been performed over a broad range in temperature, using nominally identical materials, for both types of test. It will be shown that in addition to microplasticity, as proposed by Rice [1], tensile microfracture also plays an important role in both failure processes.

2. Experimental approach

Ceramics chosen for study included sintered SiC, hot-pressed Si_3N_4, and Lucalox Al_2O_3, the properties of which are given in Table I. Both compressive and indentation specimens were prepared from identical lots of each material.

The compression test setup and precision alignment procedures have been described in detail elsewhere [2, 3], and so are outlined here only briefly. Cylindrical specimens were compressed at a strain rate of 7×10^{-5} sec^{-1}* over the temperature range −200 to 1000° C, the maximum

TABLE I Nominal ambient material properties

Material	Manufacturer/designation	Tensile strength (MPa)	DPH (GPa)	K_c ($MNm^{-3/2}$)	Grain size (μm)	T_{MP}(° C)
SiC	Carborundum/sintered α-SiC	345	28	4.4	3–5	2700
Si_3N_4	Norton/NC-132 (hot-pressed)	810	19	4.8	0.5–3	1900
Al_2O_3	General Electric/Lucalox	215	22.3	4.0	20–30	2015

*This strain rate is estimated [4] to approximate that experienced by material subjected to a two-second microhardness test.

0022–2461/83 $03.00 + .12

temperature attainable in the microhardness experiments. AD-999 alumina platens were used to test the Lucalox material, while sintered α-SiC was employed as platen material for the silicon nitride and silicon carbide. Platens and specimens were polished through 1 μm diamond grit after mating faces had been ground parallel to within 2.5 μm.

Elevated temperature microhardness tests were performed for all three materials, with specimen temperatures ranging from 23 to 1000° C. Tests were performed under an argon environment in a modified Tukon microhardness tester, with the duration of indentater–specimen contact being approximately two seconds. Hardness values were taken as the average of at least three drops each at 200, 400, 600, and 800 g, in which range the hardness was found to be load-independent. Tests at temperatures in excess of 1000° C were precluded due to deterioration of the diamond indenter. It should be noted that the sizes of the microhardness indentations in aluminium oxide were on the same scale as the grain size, whereas for SiC and Si_3N_4, the average indentation dimension was well in excess of the grain size. However, for all three materials, the plastic zone sizes of the indentations significantly exceeded the average grain size [5].

3. Results

Compressive strengths of the three ceramics as functions of temperature are shown in Fig. 1; also shown are the corresponding tensile bending strengths. From these plots, it is evident that compressive strength (σ_c) is a much more sensitive function of temperature than is tensile strength (σ_t); sintered α-SiC experiences a particularly abrupt loss of compressive strength between 500 and 800° C, while σ_t is essentially unaltered over the entire temperature range of interest.

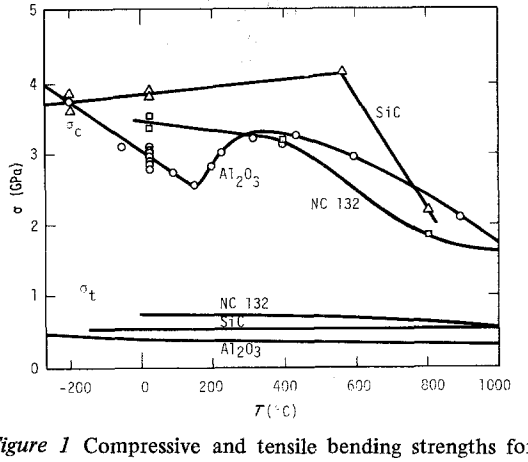

Figure 1 Compressive and tensile bending strengths for Al_2O_3, SiC, and Si_3N_4 as a function of temperature.

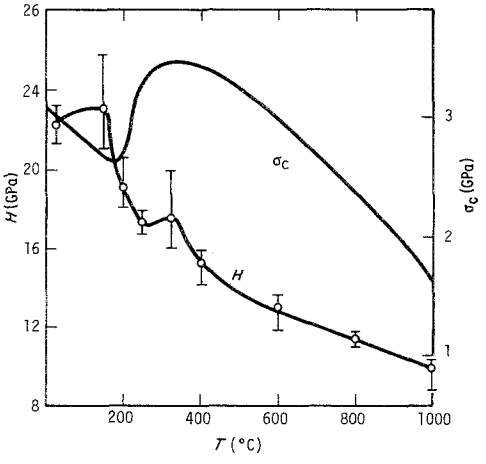

Figure 2 Hardness and compressive strength against temperature for Al_2O_3.

The relationships between hardness and temperature are shown for all three materials in Figs. 2 to 4; also shown are the preceding $\sigma_c(T)$ curves. In these representations, hardness is plotted on the left hand ordinate, and compressive strength on the right. Although the H (hardness) and σ_c curves for each material are not identical, it is evident that there are distinct qualitative similarities.

For example, superimposed on a basic trend of decreasing H and σ_c with increasing temperature are aluminum oxide hardness and strength peaks at $T \simeq 350°$ C (Fig. 2). Similarly, the down-

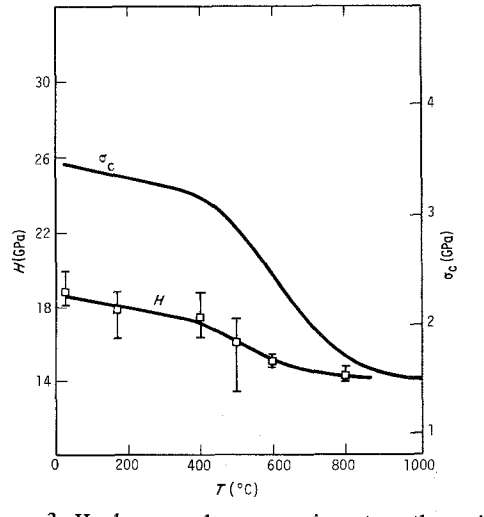

Figure 3 Hardness and compressive strength against temperature for Si_3N_4.

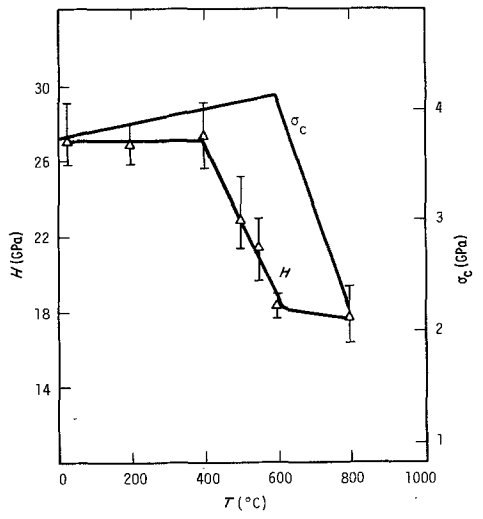

Figure 4 Hardness and compressive strength against temperature for SiC.

ward break in silicon nitride strength at $T \simeq 450°$ C (Fig. 3) is mirrored by a deflection in H at the same temperature. Finally, the extremely fast hardness drop around 400° C for silicon carbide (Fig. 4) is a precursor to the equally abrupt decrease in σ_c which ensues at $T = 600°$ C.

These similar trends in H and σ_c with temperature are reflected in microfracture similarities as well. Fractographic analysis of the compressive failure modes of these materials has been described in detail elsewhere [3, 6] by the author, and have been shown to correlate with the temperature-dependence of σ_c. For example, the sudden drop in compressive strength for SiC between 550 and 800° C corresponds to a dramatic change in fracture mode from totally transgranular to totally intergranular. Similarly, the gradual decrease in σ_c for NC 132 reflects a gradual shift from predominantly transgranular to intergranular fracture between 23 and 800° C. The behaviour of aluminum oxide is more complicated. The presence of the strength peak at 300° C is associated with enhanced twinning, which mitigates the tendency for cracking in certain grains, and enhances it in others, while the general decrease in strength from −200 to 800° C is associated with a gradual transition from predominantly transgranular to almost totally intergranular fracture.

Correspondingly, it was observed that fracture modes attending hardness indentations also appear to be temperature controlled. This is harder to see in the very fine-grained materials, but is readily apparent in Al_2O_3. Fig. 5, for example, shows indentation microfracture, for a load of 600 g, at two different temperatures. The indentation-induced cracking at 23° C (Fig. 5a) is transgranular, while at 1000° C (Fig. 5b), fracture is basically intergranular. In the latter case, the loss of entire grains is evident, as is intergranular separation elsewhere about the indent (I).

4. Discussion

It is possible to simplify the dependence of hardness upon temperature (Figs. 2 to 4) by plotting the logarithm of H against T (temperature) as

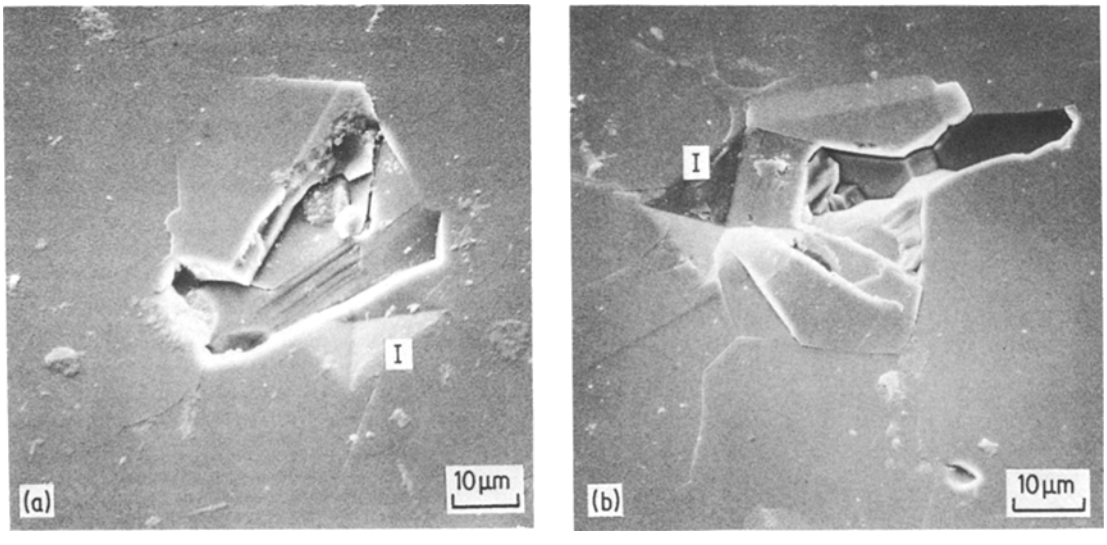

Figure 5 Indentation Fracture, Al_2O_3, Load = 600 g. I = Indentation. (a) Transgranular microfracture, $T = 23°$ C. (b) Intergranular microfracture, $T = 1000°$ C.

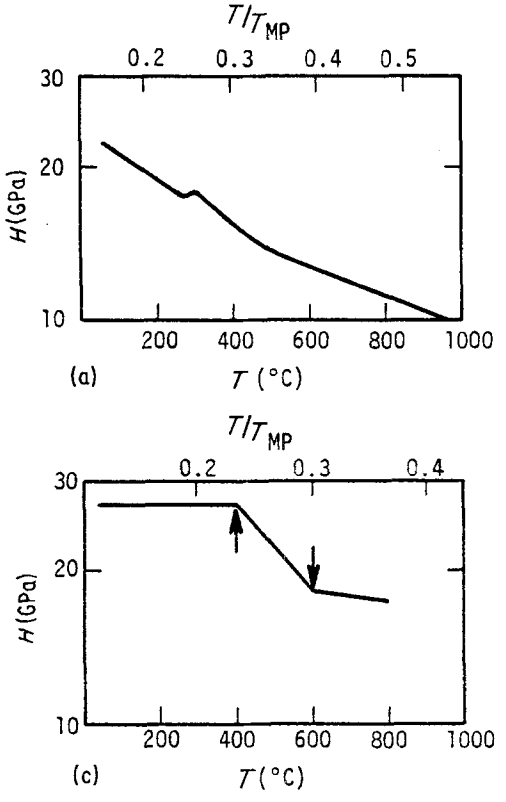

Figure 6 Semilogarithmic representation of $H(T)$, showing deviations from linearity at low homologous temperatures. (a) Al_2O_3, (b) Si_3N_4, and (c) SiC.

shown in Fig. 6. Aside from the mid-range behaviour of Al_2O_3, the curves can thus be represented by straight line segments; changes in the slopes of such segments are usually inferred to reflect changes in the fundamental damage or deformation processes. Arrows in Figs. 6b and c indicate inflection points in the log H against T curves for Si_3N_4 and SiC.

It is noteworthy that these inflections occur at rather low homologous temperatures, probably too low to correspond to fundamental changes in the dislocation processes whose increasing ease of activity with temperature is responsible for the general decrease in $H(T)$. The previously observed similarities between $\sigma_c(T)$ and $H(T)$, and the obvious correlation between sudden changes in $\sigma_c(T)$ with fractography, suggest that the inflections in $H(T)$ may have their origins in a transition from transgranular to intergranular fracture. This would mean that grain boundary failure is a significant factor in indentation plasticity at fairly low homologous temperatures. Furthermore, the author has recently shown [3, 6–8] that the compressive strength of strong ceramics is controlled by the multiple nucleation of axial tensile microcracks; the tensile stress fields responsible for the cracks arise within small regions where crystallite misorientations produce mismatched Poisson expansions. According to the preceding argument, this would suggest that the deformation-enhancing microfracture within the indentation plastic zone is tensile in nature. This hypothesis can be investigated as follows.

As Rice has pointed out [1], the yield stress $H/3$ is the upper limit of compressive strength for crystalline ceramics. Further, applications of the Griffith theory predict that the compressive strengths of ceramics should exceed their tensile strengths by a factor of at least eight, due to local tensile stresses at the tips of pre-existing flaws. Thus, it is possible to utilize $H(T)$ and $\sigma_c(T)$ to calculate theoretical corresponding tensile strengths $\sigma_t^H(T) = H(T)/24$, and $\sigma_t^c(T) = \sigma_c(T)/8$, respectively. Since σ_t^H and σ_t^c are based on $H(T)$ and $\sigma_c(T)$, they will exhibit transitions at certain temperatures, as previously observed, for $H(T)$, in Fig. 6. If the major transitions in $H(T)$ and $\sigma_c(T)$ are actually caused by transitions in tensile strength, then a critical test of the hypothesis is to show that tensile microfracture mechanisms undergo changes at the appropriate temperatures. This test can be performed by utilizing fracture-mechanism maps, recently developed by Ashby and co-workers [9, 10].

In Fig. 7, σ_t^H and σ_t^c are plotted in normalized form (σ_t/E) against temperature and homologous temperature; the slight temperature dependence of Young's modulus, E, is accounted for in the normalization procedure. The plots are superimposed on the relevant sectors of tensile fracture mechanism maps for hot-pressed silicon nitride, alumina, and hot-pressed silicon carbide [10].

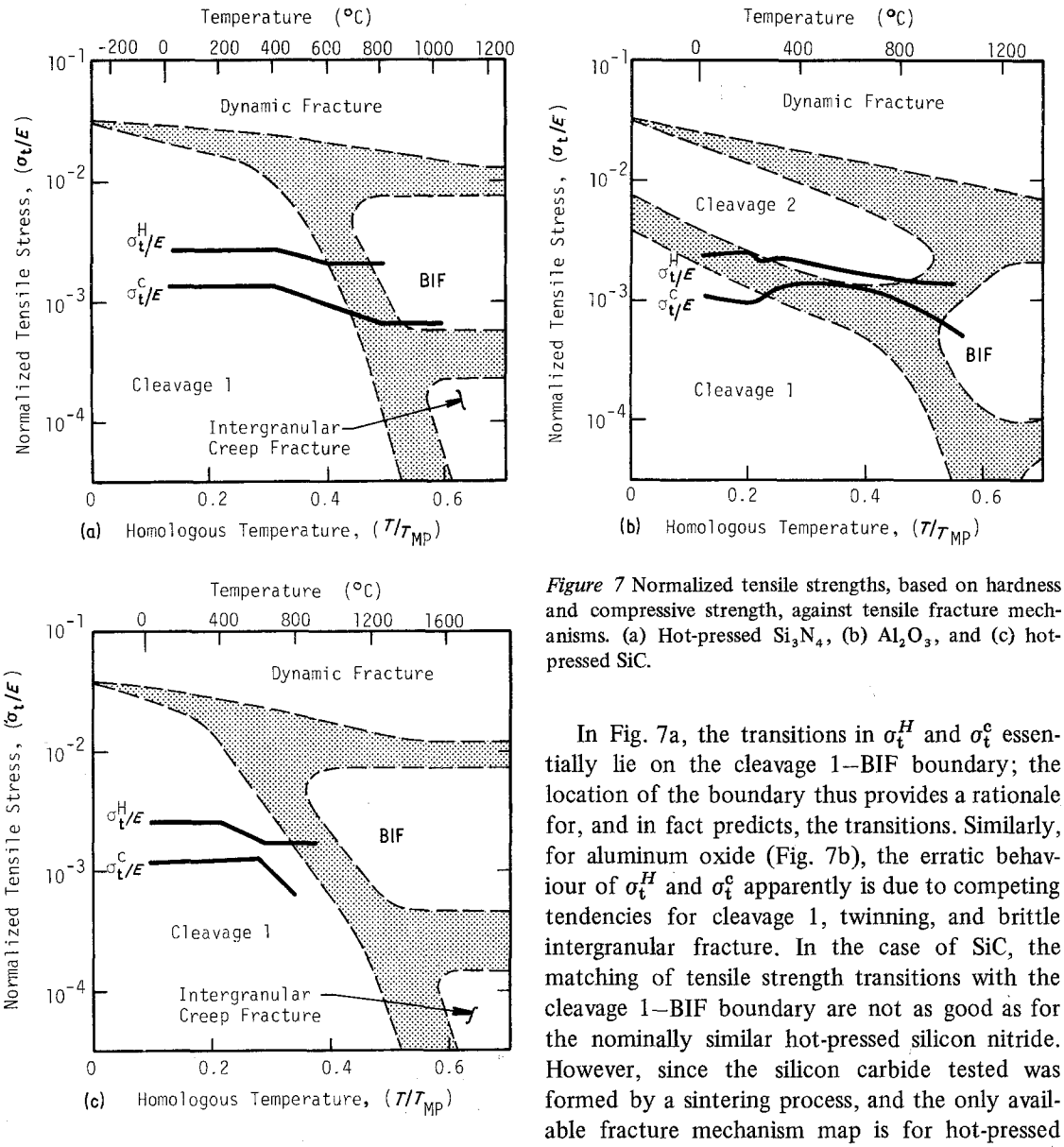

Figure 7 Normalized tensile strengths, based on hardness and compressive strength, against tensile fracture mechanisms. (a) Hot-pressed Si_3N_4, (b) Al_2O_3, and (c) hot-pressed SiC.

The three regions of the maps which are of concern here are denoted as cleavage 1, cleavage 2, and brittle intergranular fracture (BIF). The first region corresponds to the activation of pre-existing flaws or microcracks at stresses lower than those required for activation of slip or twinning systems. Cleavage 2, on the other hand, corresponds to conditions such that slip on a limited number of systems, or twinning, generate internal stresses which can nucleate cracks. Finally, brittle intergranular fracture refers to formation of a grain boundary crack due to grain boundary sliding or local plasticity. The placement of the regions is based on fractography of tensile bend specimens.

In Fig. 7a, the transitions in σ_t^H and σ_t^c essentially lie on the cleavage 1–BIF boundary; the location of the boundary thus provides a rationale for, and in fact predicts, the transitions. Similarly, for aluminum oxide (Fig. 7b), the erratic behaviour of σ_t^H and σ_t^c apparently is due to competing tendencies for cleavage 1, twinning, and brittle intergranular fracture. In the case of SiC, the matching of tensile strength transitions with the cleavage 1–BIF boundary are not as good as for the nominally similar hot-pressed silicon nitride. However, since the silicon carbide tested was formed by a sintering process, and the only available fracture mechanism map is for hot-pressed SiC, it is not surprising that the positions of the strength transitions and the fracture-mechanism boundary (Fig. 7c) fail to match perfectly. Furthermore, the extent and precise locations of the boundaries drawn by Gandhi and Ashby [10] represent subjective interpretation, as they acknowledge.

These observations suggest that it may be possible to rationalize the temperature dependence of both H and σ_c on the basis of thermally activated plasticity and temperature-controlled changes in tensile microfracture mechanisms. However, several questions immediately arise: (a) What is the meaning of three different tensile strengths, i.e. σ_t^H, σ_t^c, and σ_t, the macroscopic bend strength

shown in Fig. 1? (b) Why do σ_t^H and σ_t^c exhibit transitions, while σ_t is more or less constant over the temperature range 23 to 1000° C? (c) How is tensile microfracture involved with hardness?

The macroscopic bend strength σ_t of a ceramic generally does not represent its intrinsic tensile strength. A bend test actually uses a nominal tensile stress field to sample the initial flaw population of a specimen; failure will occur when tensile separation occurs at the most critical (size, shape) flaw. Propagation of the resulting tensile macrocrack will take place via separation modes such as cleavage and brittle intergranular fracture, which are functions of temperature. However, their influence is secondary to that of the critical flaw itself, until temperatures are sufficiently high that local plasticity is possible near the flaw, thereby increasing the fracture toughness, or the grain boundaries experience severe weakening. Over the thermal range of interest, these high temperature processes do not occur, so σ_t does not experience transitions, even though the tensile fracture mode changes.

In a compression test, failure does not take place at a single large flaw. Instead, a multitude of microscopic axial tensile cracks nucleate and eventually coalesce to cause failure [3, 7, 8]. Nucleation occurs at many sites, including both large and small intrinsic flaws, grain boundary triple points, slip band and twin intersections with grain boundaries, and at grain boundaries characterized by local modulus mismatches. Operation of the latter failure sites require higher tensile stresses than those measured in a bend test, and directly reflect the local microfracture mode, rather than flaw distributions. Thus, σ_t^c should exceed σ_t, and should exhibit transitions reflecting changes in fracture mechanism.

Similarly, hardness tests sample extremely small volumes of material, in which the probability of there residing significant numbers of flaws is even lower. Furthermore, the test is carried out under great restraint, somewhat resembling a confined pressure compression test. Tensile cracks would tend to form as a direct consequence of the operation of intrinsic tensile failure processes, which will require higher stresses than in the more global, unconfined compression test. Clearly, thermally-induced changes in microfracture mode would be expected to produce corresponding changes in σ_t^H. Thus, we should expect $\sigma_t^H > \sigma_t^c > \sigma_t$, with shifts in fracture mechanism being reflected in transitions in $\sigma_t^H(T)$ and $\sigma_t^c(T)$.

The role of tensile microfracture in compressive failure has been documented elsewhere [6–8]; not so in regard to the indentation process. In terms of the latter, we do not mean the macroscopic median–radial–lateral crack systems which have been treated in detail by Lawn *et al.* [11, 12], but rather a small zone of compression-induced tensile microfracture assumed to reside beneath a hardness indentation. This zone would contribute to indentation plasticity by facilitating the sliding and rotation of small blocks of material within the indentation plastic field, which also is characterized by high shear stresses [5]. A change in fracture mode from transgranular cleavage to brittle intergranular fracture would alter the nature of the sliding/rotation process. Further, if intergranular separation should require a lower tensile stress than does transgranular fracture, then the volume of the microfracture region, which is controlled by the stress gradient, would be larger, enhancing plasticity and lowering H.

For these hypotheses to be relevant, subsurface zones of fine-scale microfracture must actually exist at indentations. To determine if this is indeed the case, the following experiment was performed. A thin single crystal of α-SiC was indented with a Vickers diamond pyramid at various loads, with the indentation sites oriented in line across the specimen, and spaced so that the tips of their corner cracks nearly touched. The specimen was then broken in bending along this line, so that the indentation subsurface regions were revealed in section. Fig. 8a shows an SEM view of a cross section through an indentation produced by a load of 1500 g; the tip of the indentation is indicated by the large arrow. Beneath the indentation lies a heavily deformed, pyramid-shaped microfracture zone, outlined by small arrows within which lateral cracks (ℓ_c) originate. Recent experimental [13] and theoretical [5] work indicates that the zone of plastic deformation associated with the indentation is approximately three times the apparent size of the microfracture zone, and more or less hemispherical in shape [13], rather than pyramidal. Microfracture details are shown in Fig. 8b, corresponding to the righthand section of the subsurface microfracture zone of Fig. 8a, and in Fig. 8c, centred 6 μm beneath the tip of a similar indentation. Microcracks within the fracture zone tend to line up in a direction roughly

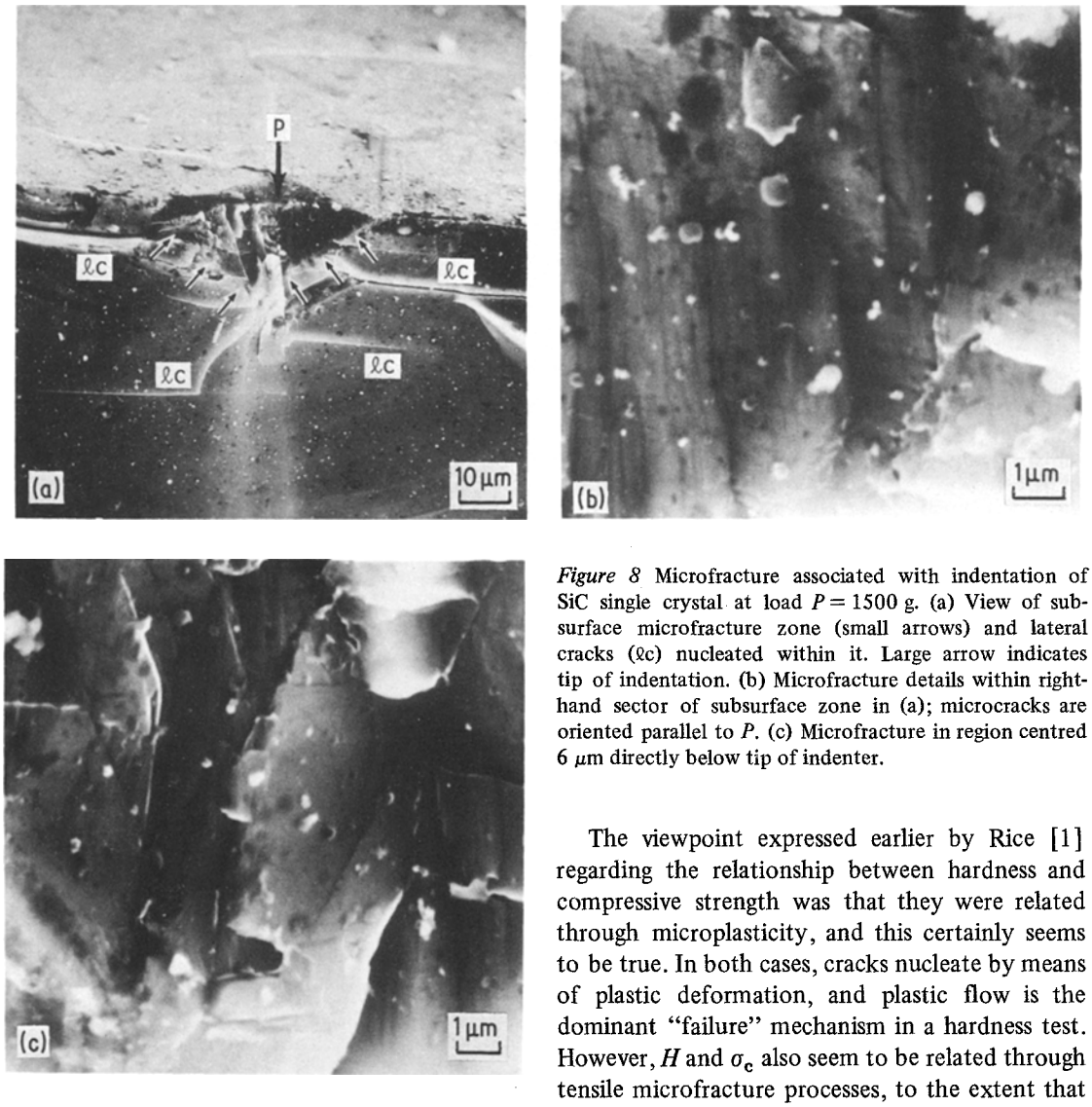

Figure 8 Microfracture associated with indentation of SiC single crystal at load $P = 1500$ g. (a) View of subsurface microfracture zone (small arrows) and lateral cracks (ℓc) nucleated within it. Large arrow indicates tip of indentation. (b) Microfracture details within right-hand sector of subsurface zone in (a); microcracks are oriented parallel to P. (c) Microfracture in region centred 6 μm directly below tip of indenter.

parallel to the indentation load axis (vertical), a situation roughly analogous to the axial microfracture pattern characteristic of compressive loading.

Actually, subsurface microfracture zones in crystalline ceramics have been observed before [14, 15], but they usually have drawn little attention. A notable exception is the recent study of CVD ZnS by Van der Zwaag *et al.* [15]; in the case of this soft, weak material, grain-boundary fracture, sliding, and accompanying porosity were so extensive that they obviously were principal contributors to indentation plasticity and macroscopic crack nucleation. The present work suggests that subsurface tensile microfracture is important in the indentation deformation of strong ceramics as well.

The viewpoint expressed earlier by Rice [1] regarding the relationship between hardness and compressive strength was that they were related through microplasticity, and this certainly seems to be true. In both cases, cracks nucleate by means of plastic deformation, and plastic flow is the dominant "failure" mechanism in a hardness test. However, H and σ_c also seem to be related through tensile microfracture processes, to the extent that a hardness test can be considered to represent a hydrostically-confined compression test of a specimen which, because of its small volume, is nearly "perfect". Since the specimen is basically flaw free, stresses are sufficiently high that extensive dislocation activity is possible throughout the "specimen", accounting for the basically monotonic decrease in H with increasing temperature. Tensile microfracture changes are responsible for transitions superimposed on the predominant plasticity effect. Compression tests, on the other hand, do not permit such high bulk stresses, microplasticity is minimized, and microfracture is the predominant factor in the material state of damage. In fact, the author has shown elsewhere [3, 8] that the thermally activated process which causes the general reduction in σ_c with increasing

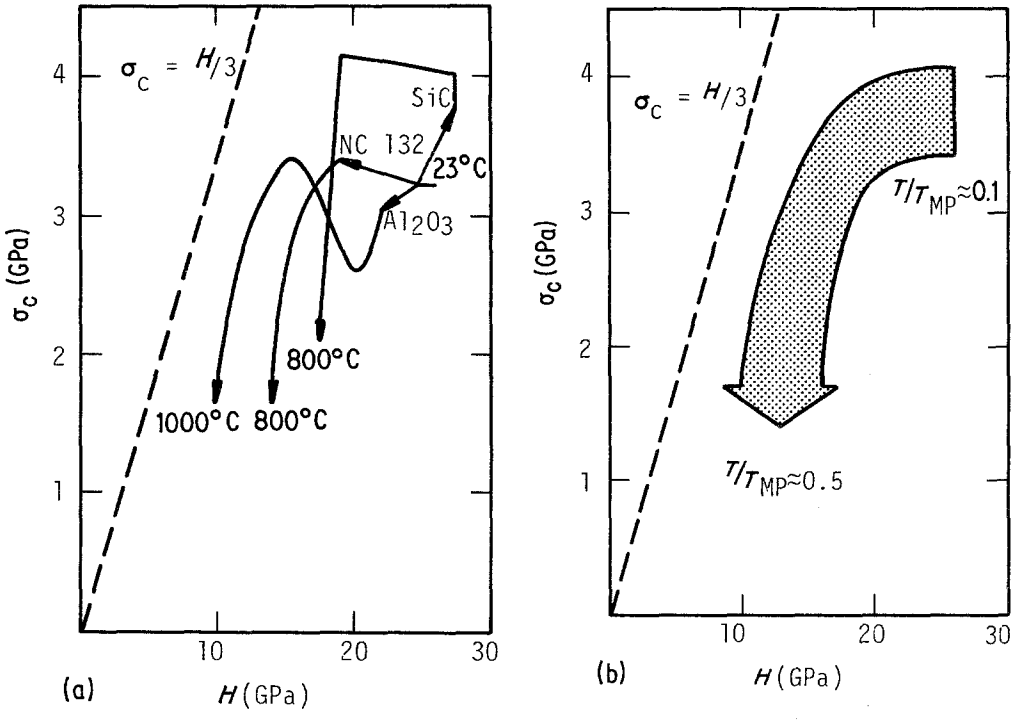

Figure 9 Effect of temperature on the relationship between yield stress ($H/3$) and compressive strength. (a) Compressive strength against hardness for Al_2O_3, SiC and Si_3N_4 as a function of temperature. (b) General trend of compressive strength against hardness and increasing homologous temperature.

temperature is enhanced subcritical growth of tensile microcracks, not enhanced plasticity. Changes in tensile microfracture mode correspond to different subcritical crack growth mechanisms, hence to the observed abrupt transitions in $\sigma_c(T)$.

Strong ceramics subject to bulk compression or to micro-indentation respond both by plastic flow and by tensile microfracture. The fundamental difference between the two tests is that in one, tensile fracture predominates, and microplasticity is secondary, while in the other, the roles are reversed. Confined bulk compression tests, and indentation at high loads, thereby sampling larger volumes of material, form links in a continuum of tests which probably afford greater balance in the relative contributions of the two damage mechanisms. If, as Rice has pointed out [1], the coupling between H and σ_c were solely a microplastic one, then it would be anticipated that at elevated temperatures, easier slip in compression should cause σ_c to approach $H/3$. As shown in Fig. 9, this is not the case in the present instance, at least for temperatures as high as $T/T_{MP} \approx 0.5$ (where T_{MP} is the melting temperature). At these temperatures, the compressive specimens fail through intergranular tensile separation before the stress level within the individual crystallites can reach $H/3$.

Macroscopic cracks which nucleate at indentations have previously been analysed [11, 12] primarily in terms of the driving force for extension following nucleation. It is thought [16] that the nuclei for radial cracks are microscopic surface flaws, and it has been shown [17] that in soda lime glass, subsurface lateral cracks nucleate at shear microcracks produced during formation of the indentation. The present results suggest that lateral cracks in strong ceramics are nucleated as a consequence of tensile microfracture within the highly stressed compressive zone just beneath the tip of the indenter. As the indentation load decreases, the volume of the high compression region decreases, and the specimen effectively becomes more "perfect"; the relative absence of microfracture at very low loads could explain the existence of a lateral crack threshold [14].

5. Conclusions

The hardness and compressive strength of strong ceramics behave in qualitatively similar fashions

to temperatures as high as $T/T_{MP} \simeq 0.5$. The bases for this similarity are microplasticity and tensile microfracture. Changes in tensile fracture mode correlate with abrupt transitions in the temperature dependence of hardness and compressive strength. Thus, subsurface indentation microfracture actually contributes to indentation plasticity, and simultaneously provides nuclei for lateral cracks. It is suggested that a hardness test can be considered as an extreme in compression testing, i.e. high confining pressure, and a more-or-less perfect specimen.

Acknowledgement

The author is grateful for the support of the Office of Naval Research under Contract No. N00014-75-C-0668.

References

1. R. W. RICE, *Mater. Sci. Res.* 5 (1970) 195.
2. J. LANKFORD, *J. Amer. Ceram. Soc.* 64 (1981) C33.
3. *Idem, J. Mater. Sci.* 16 (1981) 1567.
4. B. EVANS and C. GOETZE, *J. Geophys. Res.* 84 (1979) 5505.
5. S. S. CHIANG, D. B. MARSHALL and A. G. EVANS, *Proc. Roy. Soc.* in press.
6. J. LANKFORD, *J. Amer. Ceram. Soc.* submitted.
7. *Idem, ibid.* 62 (1979) 62.
8. *Idem*, in "Fracture Mechanics in Ceramics" Vol. 6, edited by R. C. Bradt, A. G. Evans, D. P. H. Hasselman and F. F. Lange (Plenum Press, New York, 1982) in press.
9. M. F. ASHBY, C. GANDHI and D. M. R. TAPLIN, *Acta. Metall.* 27 (1979) 699.
10. C. GANDHI and M. F. ASHBY, *ibid.* 27 (1979) 1565.
11. B. LAWN and R. WILSHAW, *J. Mater. Sci.* 10 (1975) 1049.
12. B. R. LAWN and M. V. SWAIN, *ibid.* 10 (1975) 113.
13. J. LANKFORD and D. L. DAVIDSON, *ibid.* 14 (1979) 1669.
14. A. G. EVANS and T. R. WILSHAW, *Acta Metall.* 24 (1976) 939.
15. S. VAN DER ZWAAG, J. T. HAGAN and J. E. FIELD, *J. Mater. Sci.* 15 (1980) 2965.
16. T. HARANOH, H. ISHIKAWA, N. SHINKAI, and M. MIZUHASHI, *ibid.* 17 (1982) 1493.
17. M. V. SWAIN, *J. Amer. Ceram. Soc.* 62 (1979) 318.

Received 6 September
and accepted 20 September 1982